Effect of attractive interactions on tagged particle dynamics

2003 J. Phys.: Condens. Matter 15 4657

(http://iopscience.iop.org/0953-8984/15/27/301)

INSTITUTE OF PHYSICS PUBLISHING JOURNAL OF PHYSICS: CONDENSED MATTER

J. Phys.: Condens. Matter **15** (2003) 4657–4669 PII: S0953-8984(03)60500-X

Effect of attractive interactions on tagged particle dynamics

Charanbir Kaur and Shankar P Das[1]

School of Physical Sciences, Jawaharlal Nehru University, New Delhi 110067, India

E-mail: shankar0359@yahoo.com

Received 7 March 2003
Published 27 June 2003
Online at stacks.iop.org/JPhysCM/15/4657

Abstract

We study tagged particle dynamics in a one-component simple liquid characterized by the Lennard-Jones (LJ) interaction potential. Extended mode coupling theory is used to obtain the correlation function which feeds back on the dynamics of the self-correlations. The cooperative dynamical effects are studied by evaluating various properties of tagged particle motion as influenced by the collective dynamics. Comparison between the results obtained for particles with purely repulsive interactions like the truncated LJ potential (or the hard-sphere interaction) and that of the full LJ potential are shown. The nature of the velocity autocorrelation function and the non-Gaussian variation of the van Hove self-correlation function is specifically highlighted here. The role of static structural input in the theory is considered especially in this regard.

1. Introduction

The non-exponential relaxation of the equilibrium time correlation functions in a supercooled liquid has been extensively studied using both the experimental [1, 2] and computer simulation techniques [3–6]. Many features of the tagged particle dynamics and associated dynamical heterogeneities have been measured in these studies, the major emphasis being to understand the basic mechanisms that govern the non-exponential nature of relaxation. Within a theoretical framework, the present authors [7] presented a comprehensive study of the different dynamical features of tagged particle motion that indicate the presence of dynamical heterogeneities in computer simulation studies [5, 6]. This was done using self-consistent mode coupling theory for a one-component hard-sphere (HS) system governed by Newtonian dynamics. Such studies have also been done for HS systems evolving via Brownian dynamics [8]. Thus, the theoretical tools to measure these properties have been applied mainly to systems characterized by an HS interaction potential. A step closer to real systems are those models involving attractive forces. The Lennard-Jones (LJ) 6–12 potential is the most widely studied example in this context. This

[1] Author to whom any correspondence should be addressed.

0953-8984/03/274657+13$30.00

pair potential is represented as $u(r) = 4\epsilon[(\frac{\sigma}{r})^{12} - (\frac{\sigma}{r})^{6}]$. The $u(r)$ has a steep short-range repulsive part and a longer-range attractive part. Here ϵ refers to the depth of the potential and σ is a measure of particle size. At high temperatures, the attractive part of $u(r)$ becomes almost insignificant but it plays an important role in determining the dynamics at lower temperatures. Here we consider a one-component LJ liquid in studying the role of attractive interactions in determining the nature of correlated dynamics while the system is in a supercooled state.

The self part of the van Hove correlation function $G_s(r, t)$, is a measure of the conditional probability of locating the tagged particle at a distance r from its original position in a time interval t. The $G_s(r, t)$ has a simple Gaussian variation [9] in both the limits of $t \to 0$, where free particle dynamics dominate, and in the very long-time diffusive regime. The effect of cooperative dynamics in the liquids is most evident for intermediate timescales where the $G_s(r, t)$ no longer shows a Gaussian spatial variation. The non-Gaussian parameter $\alpha_2(t)$ is the first-order correction to the Gaussian variation that is reflected in the corresponding Fourier transform of $G_s(r, t)$, given by $\psi_s(q, t)$. The $\alpha_2(t)$, defined as [9, 10]

$$\alpha_2(t) = \frac{3}{5}\frac{\langle r^4(t)\rangle}{\langle r^2(t)\rangle^2} - 1, \tag{1}$$

quantifies the effects of correlated dynamics. Its variation over the different timescales reflects the various stages of cooperative relaxation. In equation (1) $\langle r^2(t)\rangle$ and $\langle r^4(t)\rangle$ are the second- and fourth-order moments of $G_s(r, t)$, where $\langle r^2(t)\rangle$ denotes the mean square displacement of the tagged particle in time t. We evaluate these moments and hence the $\alpha_2(t)$ by calculating the self-correlation function [7]. The dynamics of a single particle in a dense fluid is invariably determined by the correlated motions of the surrounding particles in the system. The tagged particle correlation is obtained using the self-consistent mode coupling theory (MCT) [11]. We use the extended mode coupling model [12] in which the role of coupling between dominant density fluctuations as well as that between current and density fluctuations is considered for compressible liquids. The simple MCT model [13] results if such non-hydrodynamic corrections as obtained by considering the non-linear current–density couplings are ignored in the theory. This predicts that the correlations freeze beyond a critical point and an ergodic to non-ergodic dynamic transition results.

The main focus of the present work is to study the qualitative changes incurred because of the continuous and attractive nature of the interparticle potential. This is specifically studied in properties like the non-Gaussian parameter, the mean square displacement, the velocity autocorrelation function and the fraction of 'mobile particles' [5–7]. The static structural properties for the full LJ potential are also evaluated here using a much improved technique referred to as the Due–Haymet method [14]. In the next section we present the theoretical framework used for the present study, and we also describe briefly the scheme for evaluation of the static structure factor $S(k)$. In section 3 the numerical results obtained are illustrated, the implications of which are discussed in the concluding section.

2. The studied model

The self-consistent mode coupling theory (MCT) is based upon evaluating the normalized density autocorrelation function $\psi(q, t)$. The Laplace transform of $\psi(q, t)$, defined as

$$\psi(q, z) = -\mathrm{i}\int_0^\infty \mathrm{d}t\, \mathrm{e}^{\mathrm{i}zt}\psi(q, t), \qquad \mathrm{Im}(z) > 0 \tag{2}$$

is expressed in terms of the generalized memory function $\Gamma^R(q, z)$ as

$$\psi(q, z) = \frac{z + \mathrm{i}\Gamma^R(q, z)}{z^2 - \Omega_q^2 + \mathrm{i}\Gamma^R(q, z)[z + \mathrm{i}q^2\gamma(q, z)]} \tag{3}$$

in the extended mode coupling model [12, 15]. Here Ω_q corresponds to the microscopic frequency $\Omega_q^2 = q^2 v_0^2 [S(q)]^{-1}$ for the liquid state dynamics. In this, v_0 is the average thermal speed of the particle, $v_0^2 = k_B T/m$, T being the temperature of the system and m the mass of the particles. The cut-off function $\gamma(q, z)$ is obtained in the above equation as a result of the non-linear coupling between the current and density fluctuations and is responsible for restoring ergodicity. We use here its expression obtained in the one-loop approximation [15] which becomes exact in the hydrodynamic limit.

The generalized longitudinal viscosity $\Gamma^R(q, z)$ in equation (3) contains the bare and the mode coupling part, expressed as $\Gamma^R(q, z) = \Gamma^B(q) + \Gamma_{mc}(q, z)$. The uncorrelated collisions occurring during the short time are responsible for the bare contribution $\Gamma^B(q)$ to the viscosity. The bare transport coefficients have been explicitly calculated for the HS systems in terms of the particle diameter σ_{HS} and the Enskog collision time t_E using kinetic theory models. This t_E is given by $t_E = \sqrt{\beta m}/[4\sqrt{\pi} n g(\sigma_{HS})\sigma_{HS}^2]$, n being the average number density and $g(\sigma_{HS})$ the radial distribution function at σ_{HS}. We approximate the bare contributions for the LJ system by the corresponding expression for the HS system. For expressing the effective HS diameter σ_{HS} in terms of σ in the LJ case, we use σ_{HS} as that distance where the first peak appears in the corresponding radial distribution function $g(r)$ [16]. This is utilized in expressing the characteristic LJ timescale $\tau_{LJ} = \sqrt{m\sigma^2/\epsilon}$ in terms of t_E, as

$$\tau_{LJ} = 4\sqrt{\pi T^*} n^* g(\sigma_{HS}) \left[\frac{\sigma_{HS}}{\sigma}\right]^2 t_E. \tag{4}$$

Here T^* is the reduced temperature defined as $T^* = k_B T/\epsilon$. We will use this to compare the results in the case of HS and LJ systems in the next section. The inverse Laplace transform of the mode-coupling contribution $\Gamma_{mc}(q, z)$ in equation (3) is given by [12, 15]

$$\Gamma_{mc}(q, t) = \frac{n v_0^2}{2} \int \frac{\mathrm{d}\vec{k}}{(2\pi)^3} \psi(q, t)\psi(|\vec{q} - \vec{k}|, t) V(\vec{q} - \vec{k}, \vec{k}), \tag{5}$$

where the vertex function is,

$$V(\vec{q}, \vec{k}) = S(k)S(k_1)[(\hat{q} \cdot \vec{k})c(k) - \hat{q} \cdot \vec{k}_1 c(|\vec{q} - \vec{k}|)]^2, \tag{6}$$

$\vec{k}_1$ representing $\vec{q} - \vec{k}$. The input structural quantities like the static structure factor $S(k)$ and the Ornstein–Zernike direct correlation function $c(k)$ in equation (6) are determined by the interaction potential. This illustrates the role of the interaction potential in determining the correlated effects of dynamics.

The tagged particle dynamics is evaluated in terms of the self-correlation function

$$\psi_s(q, t) = \langle n^s(-q, 0) n^s(q, t) \rangle, \tag{7}$$

where tagged particle density $n^s(q, t) = \mathrm{e}^{-\mathrm{i}\vec{q} \cdot \vec{R}(t)}$. The self-consistent dynamical equation for the Laplace transform of $\psi_s(q, t)$ in the standard mode coupling model [11] is given as

$$\psi_s(q, z) = \frac{z + \mathrm{i}\Gamma_s^R(\vec{q}, z)}{z^2 - v_0^2 q^2 + \mathrm{i}z\Gamma_s^R(\vec{q}, z)}. \tag{8}$$

This is obtained [11] by considering the generalized fluctuating hydrodynamic equations for the tagged particle motions. In this equation, the bare contribution to the memory function, Γ_B^s, is also approximated by the corresponding HS expression as discussed above in the case of collective correlations. The mode coupling effects in the dynamical relaxation are described by the quantity $\Gamma_{mc}^s(q, t)$ which is obtained as a coupling between the self and collective correlations as [11]

$$\Gamma_{mc}^s(q, t) = n v_0^2 \int \frac{\mathrm{d}\vec{k}}{(2\pi)^3} V_s(\vec{q} - \vec{k}, \vec{k}) \psi(k, t) \psi_s(|\vec{q} - \vec{k}|, t) \tag{9}$$

with the vertex function

$$V_s(\vec{q}-\vec{k},\vec{k}) = (\hat{q}\cdot\vec{k})^2[c(k)]^2 S(k). \tag{10}$$

To evaluate the non-Gaussian parameter $\alpha_2(t)$ in this model, the $\psi_s(q,t)$ is calculated in the small-q range by expressing $\Gamma_s^{mc}(q,t)$ in a Taylor series expansion up to $O(q^2)$, such that from equation (8) the $\psi_s(q,t)$ is expressible as a cumulative expansion [9] up to $O(q^4)$. This is evaluated for ten values of $q\sigma$ in the range from 0.01 to 0.1, which is small enough for the quantity $\frac{1}{q^2}[1-\psi_s(q,t)]$ to have a linear variation with q^2. The slope of this linear variation is $-\frac{1}{120}\langle r^4(t)\rangle$ and the intercept $\frac{1}{6}\langle r^2(t)\rangle$ [9], from which the corresponding $\alpha_2(t)$ is obtained using equation (1). The details regarding the form of the coefficients in the Taylor expansion of Γ_s^{mc} etc will be published elsewhere.

2.1. Static structure factor

The information regarding the interaction potential $u(r)$ of the system is implicitly used to obtain the solution of the above dynamical equations through the static structure factor $S(k)$ and the direct correlation function $c(k)$. To obtain these for the LJ potential we mainly follow the scheme of Due and Haymet [14] which we briefly describe in this section.

In general, the Ornstein–Zernike equation [17] defines the relation between the direct correlation function $c(r_{12})$ between particles at a distance $r_{12} = |\vec{r}_1 - \vec{r}_2|$ and the total correlation function $h(r_{12}) = g(r_{12}) - 1$, where $g(r)$ is the pair correlation function. This relation is given as

$$h(r_{12}) = c(r_{12}) + n\int \mathrm{d}\vec{r}_3\, c(r_{13})h(r_{32}). \tag{11}$$

For a spherically symmetric, pair-wise additive potential, these static correlation functions are related to the interaction potential by the exact relation [17]

$$h(r) = \exp[-\beta u(r) + h(r) - c(r) + B(r)] - 1. \tag{12}$$

Here $B(r)$ represents the sum of all bridge diagrams or the 'bridge function' for the potential $u(r)$. An appropriate approximation to this function $B(r)$ in terms of either $c(r)$ or $h(r)$ constitutes a closure to the above two equations which can then be solved to obtain the structural properties.

In perturbation theories [18, 19], the LJ interaction potential is partitioned into a reference potential $u_1(r)$ and a perturbation $u_2(r)$. This $u_2(r)$ is approximated in the Due–Haymet scheme [14] as a density-dependent function

$$u_2(r) = -4\epsilon\left(\frac{\sigma}{r}\right)^6 \exp\left[\frac{-\epsilon}{n^*}\left(\frac{\sigma}{r}\right)^6\right] \tag{13}$$

using a semi-phenomenological approach. This is used to define the function $s(r) = h(r) - c(r) - \beta u_2(r)$, in terms of which the Bridge function is formulated as

$$B(r) \approx B(s) = \frac{-s^2}{2\left[1+\left(\frac{5s+11}{7s+9}\right)s\right]}. \tag{14}$$

Using the above closure, the two equations (11) and (12) are solved iteratively to finally obtain the relevant correlation functions and the corresponding Fourier transforms.

3. Results

We illustrate here some features of tagged particle dynamics in case of a one-component LJ liquid. We compare the dynamical features of the LJ liquid with systems governed by purely repulsive interactions, in order to study the effects of attractive forces on the dynamics. For this we consider (a) the HS system and (b) the system characterized by the so-called cut LJ potential. The form for truncated LJ potential is taken such that purely repulsive part of full LJ potential is considered and is formulated as,

$$u(r) = \begin{cases} 4\epsilon\left[\left(\frac{\sigma}{r}\right)^{12} - \left(\frac{\sigma}{r}\right)^{6}\right] + \epsilon, & r \leqslant r_0 \\ 0, & r > r_0 \end{cases} \tag{15}$$

truncated at $r_0 = 2^{1/6}\sigma$ where the full LJ potential shows the minimum of the potential well. This form of the potential makes it most appropriate to compare between the dynamical features of the full LJ system. For illustration of the form of the full LJ and cut LJ potential see the inset of figure 3. To obtain the static structure factor for the truncated LJ potential, we have computed the equivalent HS diameter [18] and used the Percus–Yevick solution with Verlet–Weiss correction added [20] to obtain the structure factor for the corresponding HS system. The effect of the static structural properties is significant here since these structural inputs to the present theory are implicitly detrimental to the subsequent dynamical relaxation in dense liquids.

In figure 1 we illustrate the variation of the $S(k)$ with the wavevector $k\sigma$ at the reduced temperature $T^* = 0.723$ ($T^* = k_BT/\epsilon$) and density $n^* = 0.999$ ($n^* = n\sigma^3$), as obtained by the Due–Haymet scheme [14] described in section 2.1. The $S(k)$ for the same full LJ potential, obtained by the standard WCA scheme [18, 19], is also shown in this figure as the dashed curve for comparison. The corresponding comparison of the radial distribution function $g(r)$ is shown as the inset to this figure. The main differences in $S(k)$ occur at the shorter k values, i.e. larger length scales. The height of the first peak of the structure factor ($S(k)_{max}$) is also larger for the $S(k)$ obtained using the WCA technique. Due to this difference in the heights of $S(k)_{max}$, the 'ideal transition' that follows from the simple mode coupling theory [13, 21] occurs at a *lower* temperature $T_c^* = 0.695$ with this improved structure factor. The reduction in the transition temperature is by about 20% from that obtained using the WCA $S(k)$ [22].

The dynamic properties are obtained here using both the extended mode coupling theory [12] and the simple MCT model [13]. For the finite wavevector calculations, we rescale γ by a factor δ which finally determines the α relaxation timescale. The simple version of the MCT model [13] results if the cut-off function γ is ignored or equivalently if δ vanishes. This involves fixing a relevant value of the scaling factor δ such that it determines the appropriate α relaxation timescale as expected from computer simulation models.

3.1. Simple MCT results

Here we present the results evaluated using the simple mode coupling model, where the cut-off function γ is ignored in equation (3). Using this model, we will describe here both the short- and long-time dynamical features of the tagged particle motions. However, it should be noted that the short-time features are unchanged using the extended model equations as well.

3.1.1. Non-Gaussian parameter. In figure 2, we specifically focus on the short-time correlated dynamics that is indicated by the strong peak of $\alpha_2(t)$ in the HS systems [7].

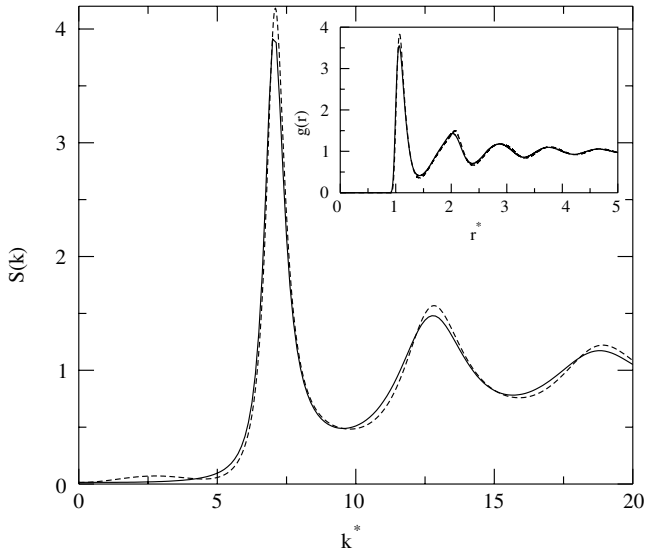

Figure 1. Static structure factor $S(k)$ at $T^* = 0.723$, $n^* = 0.999$ for the LJ potential using the Due–Haymet scheme. The dashed curve represents the $S(k)$ evaluated using the WCA technique at the same T^* and n^*. The inset shows the corresponding curves for the radial distribution function $g(r)$. Here $k^* = k\sigma$ and $r^* = r/\sigma$.

We illustrate here the $\alpha_2(t)$ for the full LJ system at temperature $T^* = 0.723$ and density $n^* = 0.999$, shown as the solid curve. We have fixed the upper limit of the wavevector integrals as $\Lambda = 50\sigma^{-1}$ with the wavevector grid size $0.1\sigma^{-1}$ here. The specification of Λ at a relatively large value is important to obtain numerically consistent results in the short-time regime. The dot dashed curve in figure 2 exhibits the $\alpha_2(t)$ for the cut LJ system at temperature $T^* = 1.145$ and density $n^* = 1.06$. The HS results at $n^* = 1.05$ are shown in the figure as the double-dot dashed curve. We choose the corresponding density and temperature for the two systems by matching the height of the first peak of respective $S(k)$'s with that obtained for the full LJ system. For direct comparison between the three systems, we have illustrated these results with the time rescaled with respect to time t_E, as discussed in section 2. This figure shows that the purely repulsive, discontinuous potential results in maximum heterogeneity at the shorter times as compared with the other two cases. This difference is due to the much faster decay of the $S(k)$ for the full LJ system at the smaller length scales or equivalently larger k values, as compared to that for the other two purely repulsive systems. This is despite matching at the respective peaks of the structure factor for the three systems. The variation of the structure at shorter length scales especially affects the shorter-time properties. Here we would like to indicate that the free-particle behaviour of the tagged particle as expected from the Newtonian dynamics is not observable in the mode coupling model due to the generalized *hydrodynamic* nature of mode coupling equations. Thus the $\alpha_2(t)$ instead of going to zero in the limit $t \to 0$, converges to a constant value $-2/3$ as can be obtained analytically from the linearized equation for the tagged particle correlator.

In figure 3 we show the long-time behaviour of $\alpha_2(t)$ corresponding to the LJ, HS and the truncated LJ potential. We fix the thermodynamic parameters for the three systems by matching the first peak of $S(k)$. Using this criterion, the comparison is made w.r.t. the LJ system at $T^* = 1.10$ and the cut LJ system at $T^* = 1.60$, both for the density $n^* = 0.999$. The corresponding results for the HS system are obtained at a density $n^* = 0.985$. We have chosen

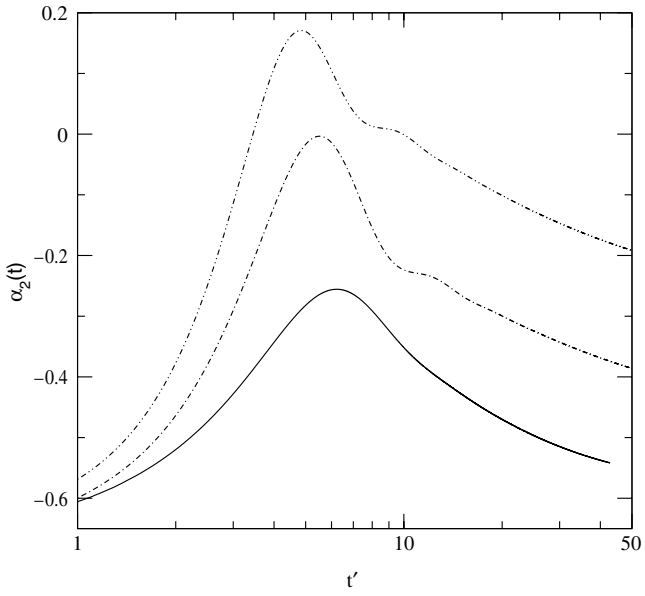

Figure 2. Comparison of the non-Gaussian parameter $\alpha_2(t)$ at short time for full LJ system (solid curve) at $T^* = 0.723$, $n^* = 0.999$ with the cut LJ system (dot dashed) at $T^* = 1.145$, $n^* = 1.06$ and the HS system at $n = 1.05$ (double-dot dashed curve). The $\alpha_2(t)$ is plotted against dimensionless time $t' = t/t_E$ (see text for t_E).

here a comparatively higher temperature range in order to evaluate the long-time features within a computationally viable time span. We observe that the timescale of relaxation with the purely repulsive potentials is larger than for the full LJ system. The peak height of $\alpha_2(t)$ is also largest for the HS system which is similarly observed for the short-time peak. These results are obtained here by fixing $\Lambda = 25.0\sigma^{-1}$. It appears that the large-time features for the dynamics are less sensitive to the upper cut-off Λ. To evaluate the long-time dynamics we thus choose a comparatively smaller value for Λ in this numerical calculation. In the inset of this figure we illustrate the comparative nature of the interaction potentials. The solid curve shows the full LJ potential and the dot dashed curve depicts the cut LJ potential.

3.1.2. Velocity autocorrelation function and $G_s(r, t)$. Another significant difference observed in the dynamical properties due to change in the structure concerns the velocity autocorrelation functions $\psi_v(t)$ for the three cases. We evaluate $\psi_v(t)$ as [9]

$$\psi_v(t) = \frac{1}{6v_0^2}\frac{\mathrm{d}^2}{\mathrm{d}t^2}\langle r^2(t)\rangle. \tag{16}$$

The negative-time tail of $\psi_v(t)$ is a characteristic feature of dense liquid dynamics. It physically illustrates the *back-scattering* effects typically produced due to the rattling motion of the particle while being trapped in the cage formed by the surrounding particles. We show in figure 4, that the discontinuous, repulsive nature of the HS potential results in a marked oscillatory decay of $\psi_v(t)$ as compared with its almost monotonically vanishing negative tail in the LJ liquid. For the truncated LJ potential, the $\psi_v(t)$ also shows an oscillation, though with a much smaller amplitude. The results shown here correspond to the same thermodynamic parameters as used to obtain the short-time behaviour of $\alpha_2(t)$ in figure 2.

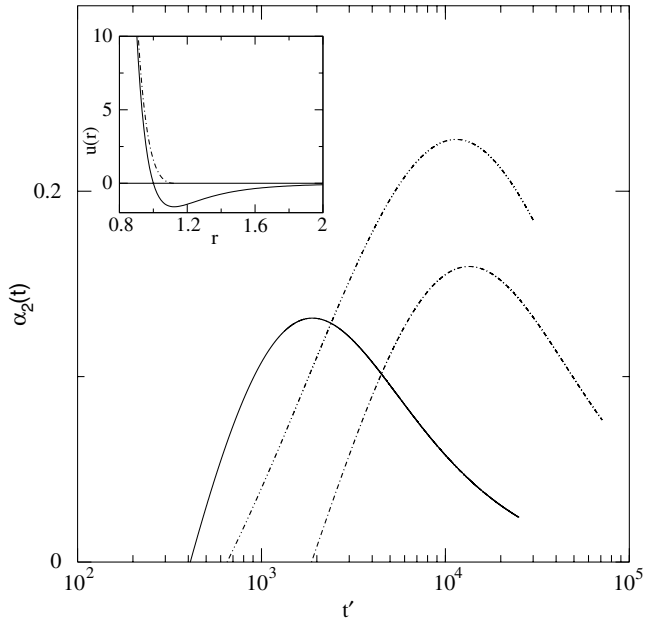

Figure 3. The comparison of the non-Gaussian parameter $\alpha_2(t)$ at long times using the simple MCT model for the full LJ system (solid curve), cut LJ potential (dot dashed curve) and the HS system (double-dot dashed curve). These results are obtained with $T^* = 1.10$ (LJ), $T^* = 1.60$ (cut LJ) at $n^* = 0.999$ and at $n^* = 0.985$ for the HS system. The inset shows the relative comparison between the full LJ potential (solid curve) with the purely repulsive cut LJ potential (dot dashed curve).

In figure 5 we illustrate the variation of the probability $4\pi r^2 G_s(r,t)$ with distance r at time t_{p2}, at which the non-Gaussian parameter shows its maximum in the later-time regime (figure 3). This figure illustrates the non-Gaussian nature of the van Hove self-correlation function on comparison with the corresponding Gaussian function $G_s^0(r,t)$, shown as the dot dashed curve for both the cut LJ system (main figure) and the full LJ system (as inset) for the same n^* and T^* as used to obtain figure 3. The $G_s^0(r,t)$ is evaluated as $G_s^0(r,t) = [3/(2\pi\langle r^2(t)\rangle)]^{\frac{3}{2}} \exp(-3r^2/2\langle r^2(t)\rangle)$ at the corresponding time, using the computed value of $\langle r^2(t)\rangle$. The stretched variation of $G_s(r,t)$ reflects the effects of correlated dynamics in the supercooled liquid. The point marked by the arrow indicates the distance beyond which the probability of locating the particle increases as compared with that predicted by the simple Gaussian function. In the computer simulation studies of [5, 6], such particles that cross this distance, denoted as r_M, are referred to as 'mobile particles'. In the present calculation, we obtain almost the same value of r_M as well as the corresponding fraction of mobile particles [7] for both systems considered here.

3.2. Extended MCT results

The simple MCT model predicts the 'ideal transition', marking a transition from the ergodic to a non-ergodic state at densities much smaller than that predicted by the computer simulation results [23]. In the extended MCT, the role of cut-off function γ (equation (3)) keeps the system ergodic at all densities. However, as discussed in section 2 the expression for γ is obtained up to one loop order that becomes exact only in the hydrodynamic limit. For the finite wavevector

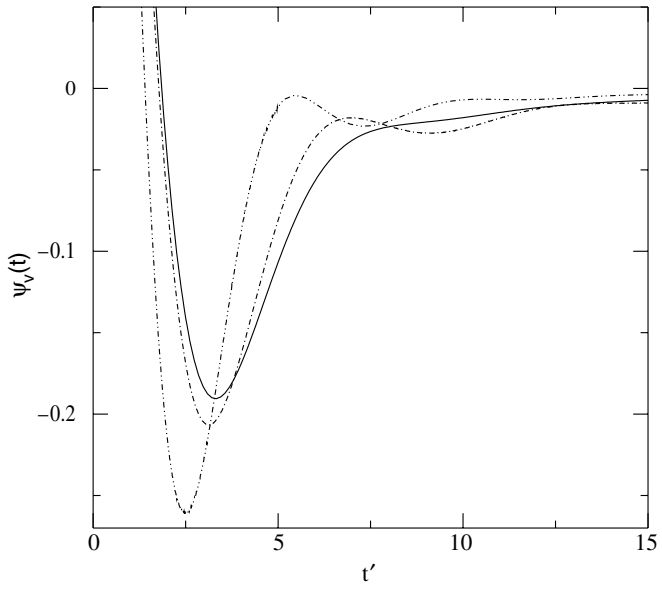

Figure 4. The velocity autocorrelation function $\psi_v((t)$ versus t' for the LJ system (solid curve), cut LJ system (dot dashed curve) and HS system (double-dot dashed curve) corresponding to the same thermodynamic parameters as used for figure 2.

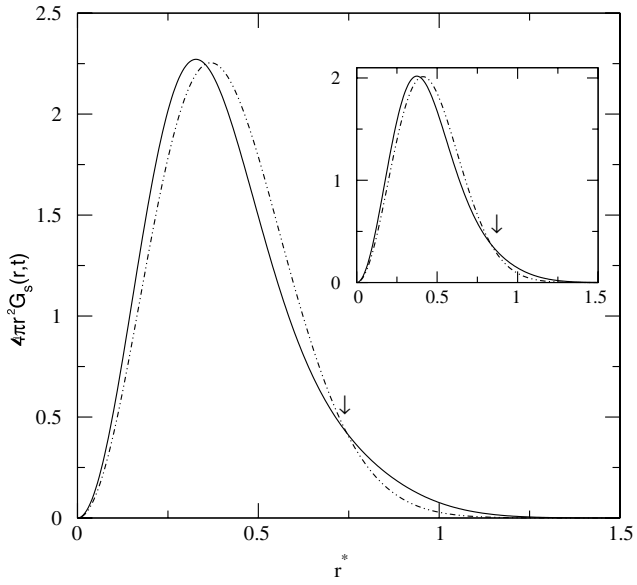

Figure 5. $4\pi r^2 G_s(r,t)$ versus $r^* = r/\sigma$ for LJ liquid evaluated at at time t_{p2} using the simple MCT model The dot dashed curves are the corresponding Gaussian distribution function $G_s^0(r,t)$. The inset illustrates the results for the cut LJ system. These are obtained using the same T^* and n^* as used to obtain figure 3.

generalization we use an overall scaling factor of δ with γ. This δ is treated in the theory as the single parameter to match the relaxation of the density autocorrelation function with the

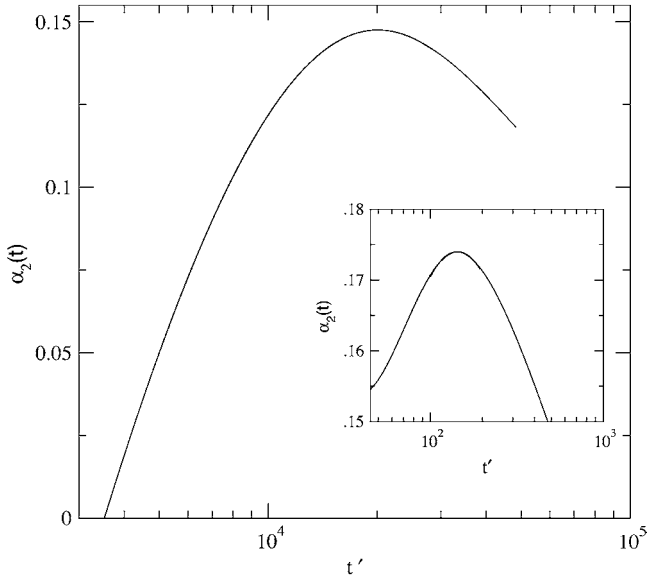

Figure 6. Non-Gaussian parameter $\alpha_2(t)$ versus time $t' = t/t_E$ for the LJ liquid at $T^* = 0.723$, $n^* = 0.999$ in the long-time range using the extended MCT model. The HS result is shown in the inset at density $n^* = 1.05$.

computer simulation results. The tagged particle correlations are then evaluated using this $\psi(q, t)$ (equation (9)).

Here, we estimate δ for the LJ system such that the shear viscosity of the system computed using the expression [24]

$$\eta = \frac{n^2 k_B T}{60\pi^2} \int \mathrm{d}t \int \mathrm{d}k\, k^4 [c'(k)]^2 S^2(k) [\psi(k, t)]^2 \tag{17}$$

in the MCT agrees with the corresponding value reported in [25]. Here, $c'(k)$ represents the first-order k derivative of $c(k)$. In [25], the transport properties of a dense one-component LJ liquid were evaluated using a master equation approach to study the dynamics in the configuration space with different minima in the potential energy landscape. The dynamics are evaluated by ignoring the crystal minima due to which the usual problem of crystallization encountered in molecular dynamics simulation of a one-component system is avoided. The dynamics in the MCT is also formulated based on the analogous assumption that crystallization does not take place. Hence, the results from such dynamical models [25] have a strong appeal for being considered with MCT. Using this criterion of fixing δ, we obtain in figure 6 the $\alpha_2(t)$ in the longer-time relaxation regime at temperature $T^* = 0.723$ and density $n^* = 0.999$ for the LJ system.

For comparison, we have shown in the inset of figure 6 the time variation of the $\alpha_2(t)$ for the HS system at density 1.05. This density is chosen such that the respective peak value of the structure factor $S(k)$ is same in both the cases. In obtaining this result for HS with extended MCT, the quantity δ for the final relaxation of the density correlation function is fixed such that the self-diffusion coefficient calculated from the theory matches with that of the molecular dynamics simulation results of [23] (as done in [7]). These results are shown for both systems with respect to the time rescaled by the Enskog collision time t_E. The heights of the respective peaks in $\alpha_2(t)$ are almost similar, with the HS fluid still showing a higher value, though the

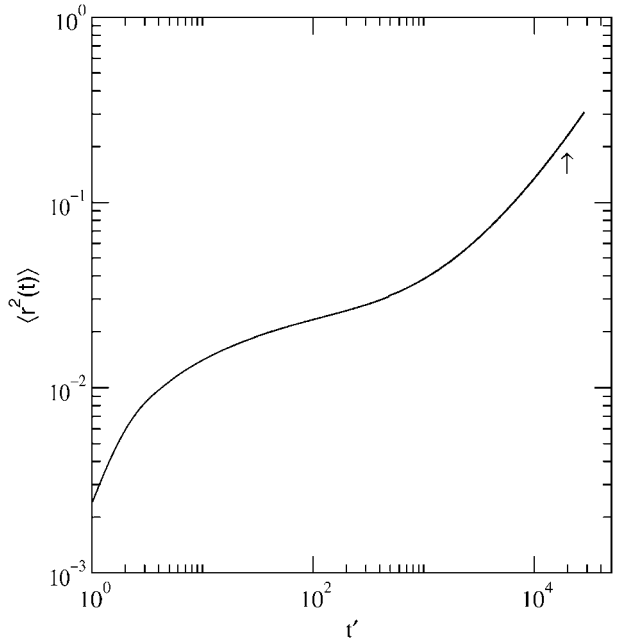

Figure 7. Variation of the mean square displacement $\langle r^2(t)\rangle$ with time t' for the LJ system at $T^* = 0.723$, $n^* = 0.999$ using the extended MCT model.

timescale of occurrence in the LJ case is much larger than that for HS. This is presumably due to the fixing of the cut-off parameter δ, determining the final timescale of relaxation in both cases. δ in both systems is fixed by matching the available computer simulation data on two different transport properties, also obtained from two different approaches [23, 25]. In figure 7 the dynamic variation of the mean square displacement $\langle r^2(t)\rangle$ for this LJ system is shown. The plateau region is indicative of the restricted motion of the tagged particle illustrating the 'cage effect'. The arrow on this curve indicates the timescale where the peak in the $\alpha_2(t)$ appears in figure 6, after which the $\alpha_2(t)$ starts decreasing. The tagged particle motion becomes purely diffusive when finally the $\alpha_2(t)$ vanishes in the very long-time limit, correspondingly the $\langle r^2(t)\rangle$ shows a linear variation with time in those timescales. In figure 8 we illustrate the variation of the probability $4\pi r^2 G_s(r, t)$ with distance r at time t_{p2}. Here also we compare for the LJ and HS system the non-Gaussian nature of the van Hove self-correlation function with the corresponding Gaussian function $G_s^0(r, t)$, shown as the dot dashed curve for both the LJ system (main figure) and the HS system (inset). The width of the probability distribution is larger in the case of the LJ system as compared with that of the HS system. This is mainly as a result of the much larger value of t_{p2} for the LJ case. This results in a widening of the probability distribution curve, an effect which is also reflected in the corresponding larger value of the mean square displacement. The fraction of 'mobile particles' is also found to be similar in both cases.

4. Discussion

Different aspects of tagged particle dynamics are studied here in the self-consistent MCT model. This work demonstrates the role of the interaction potential in determining the nature

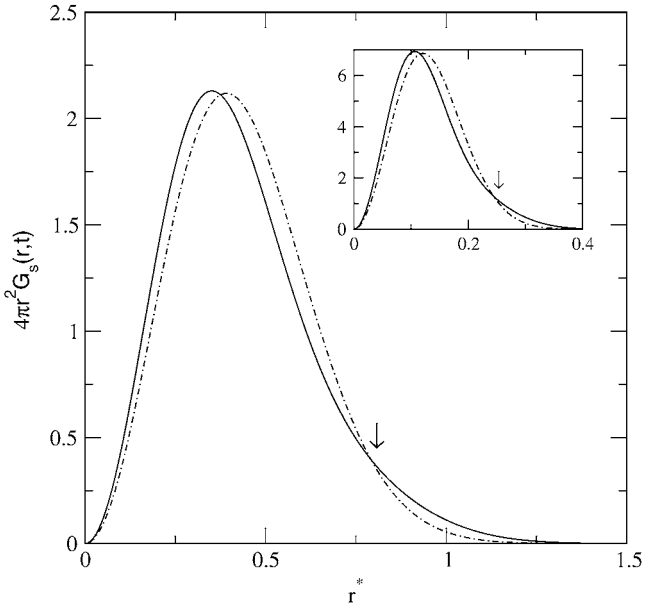

Figure 8. $4\pi r^2 G_s(r, t)$ versus $r^* = r/\sigma$ for an LJ liquid at $T^* = 0.723$, $n^* = 0.999$ at time t_{p2}. The corresponding HS result is shown as the inset at density $n^* = 1.05$. The dot dashed curves are the corresponding Gaussian distribution function $G_s^0(r, t)$.

of dynamic relaxation in dense liquid states. The non-Gaussian parameter $\alpha_2(t)$ quantifies the effect of correlated dynamics over different timescales. In the HS systems it has been found using the self-consistent MCT [7] that the $\alpha_2(t)$ shows a double-peaked structure, the first peak occurring over the shorter timescales in the β relaxation regime and the second peak in the larger α relaxation timescales. Such a two-peaked structure of $\alpha_2(t)$ has also been observed in computer simulation studies of charged colloidal systems [4] and soft-sphere alloys [3]. We have found here that the strength of the shorter-time peak decreases considerably in the case of an LJ liquid as compared with the other two systems with purely repulsive interactions. The longer-time peak shows almost the same peak height in the three cases. The HS fluid, however, shows the maximum heterogeneity. In the extended MCT calculation, the timescale of the second peak is determined by the parameter δ that has been fixed here using the computer simulation models. The difference in the shorter-time peaks in $\alpha_2(t)$ is indicative of the structural differences over small length scales.

The time variation of the velocity autocorrelation function provides a direct means of studying tagged particle motion. By evaluating this, we directly probe those features of dynamical behaviour that are most sensitive to the details of interactions. These are particularly relevant over the shorter timescales and the qualitative differences between the nature of the dynamic variation of the $\alpha_2(t)$ in this time range reflects these facts. The distinct oscillatory character of the $\psi_v(t)$ for the HS system as compared with the almost monotonic loss of the negative correlation in the LJ system depicts the different relaxation mechanisms prevailing in the two systems. The maximum negative value of $\psi_v(t)$ corresponds to the HS system. However, the LJ system shows the largest overall negative area under the curve. This shows that the corresponding diffusion (obtained as the time integral of $\psi_v(t)$) is slower for the LJ system. Thus this work shows on the basis of standard MCT model how the static structure

of the system is directly responsible for the type of dynamical heterogeneity that marks the system over different timescales.

Acknowledgments

The authors acknowledge Hahn Méitnér Institüt, Berlin for providing computational facilities. CK acknowledges financial support from the University Grants Commission and Council for Scientific & Industrial Research, India.

References

[1] Cicerone M T and Ediger M D 1995 *J. Chem. Phys.* **103** 5684
[2] Schmidt-Rohr K and Spiess H W 1991 *Phys. Rev. Lett.* **66** 3020
[3] Bernu B, Hansen J P, Hiwatari Y and Pastore G 1987 *Phys. Rev.* A **36** 4891
[4] Sanyal S and Sood A K 1998 *Phys. Rev.* E **57** 908
[5] Kob W, Donati C, Plimpton S, Poole P H and Glotzer S C 1997 *Phys. Rev. Lett.* **79** 2827
[6] Donati C, Douglas J F, Kob W, Plimpton S J, Poole P H and Glotzer S C 1998 *Phys. Rev. Lett.* **80** 2338
[7] Kaur C and Das S P 2002 *Phys. Rev. Lett.* **89** 085701
[8] Fuchs M, Götze W and Mayr M R 1998 *Phys. Rev.* E **58** 3384
[9] Boon J P and Yip S 1991 *Molecular Hydrodynamics* (New York: Dover)
[10] Rahman A 1964 *Phys. Rev.* **136** A405
[11] Kirkpatrick T R and Nieuwoudt J C 1986 *Phys. Rev.* A **33** 2658
[12] Das S P and Mazenko G F 1986 *Phys. Rev.* A **34** 2265
[13] Bengtzelius U, Götze W and Sjölander A 1984 *J. Phys. C: Solid State Phys.* **17** 5915
[14] Due D M and Haymet A D J 1995 *J. Chem. Phys.* **103** 2625
[15] Das S P 1990 *Phys. Rev.* A **42** 6116
[16] Dzugutov M 1996 *Nature* **381** 137
[17] Hansen J P and McDonald I R 1976 *Theory of Simple Liquids* (London: Academic)
[18] Weeks J D, Chandler D and Andersen H C 1971 *J. Chem. Phys.* **55** 5422
[19] McQuarrie D A 1976 *Statistical Mechanics* (New York: Harper and Row)
[20] Henderson D and Grundke E W 1975 *J. Chem. Phys.* **63** 601
[21] Bengtzelius U 1986 *Phys. Rev.* A **33** 3433
[22] Kaur C, Srivastava S and Das S P 2002 *Phys. Lett.* A **300** 291
[23] Woodcock L V and Angell C A 1981 *Phys. Rev. Lett.* **47** 1129
[24] Kirkpatrick T R and Nieuwoudt J C 1986 *Phys. Rev.* A **33** 2651
[25] Angelani L, Parisi G, Ruocco G and Villiani G 1998 *Phys. Rev. Lett.* **81** 4648